Metallothionein prolongs survival and antagonizes senescence-associated cardiomyocyte diastolic dysfunction: role of oxidative stress

Xiaoping Yang,* Thomas A. Doser,* Cindy X. Fang,* Jennifer M. Nunn,* Rajiv Janardhanan,* Meijun Zhu,† Nair Sreejayan, Mark T. Quinn,‡ and Jun Ren*,[1]

*Division of Pharmaceutical Sciences and Center for Cardiovascular Research and Alternative Medicine, and †Department of Animal Science, University of Wyoming, Laramie, Wyoming, USA; and ‡Department of Veterinary Molecular Biology, Montana State University, Bozeman, Montana, USA

To read the full text of this article, go to http://www.fasebj.org/cgi/doi/10.1096/fj.05-5288fje

SPECIFIC AIMS

Senescence is accompanied by oxidative stress and cardiac dysfunction, although the link between the two remains unclear. This study examined the role of antioxidant metallothionein on cardiomyocyte function, superoxide generation, the oxidative stress biomarker aconitase activity, cytochrome *c* release, and expression of oxidative stress-related proteins, such as the GTPase RhoA and NADPH oxidase protein $p47^{phox}$ in young (5–6 mo) and aged (26–28 mo) FVB wild-type and cardiac-specific metallothionein transgenic mice.

PRINCIPAL FINDINGS

1. Metallothionein mice showed longer life span than FVB mice evaluated by the Kaplan-Meier survival curve

The Kaplan-Meier survival curve shows that metallothionein transgenic mice display a ~4 mo longer life span compared with FVB mice. The two curves start to separate from each other after 20 mo of age with metallothionein mice exhibiting a reduced mortality rate.

2. Aging-induced cardiac contractile defects were prevented by metallothionein

The mechanical and intracellular Ca^{2+} defects triggered by advanced age have been well documented but limited research focuses on single cardiomyocytes. We assessed mechanical properties of ventricular myocytes using a SoftEdge MyoCam system. The aging-induced prolongation of time-to-90% relengthening (TR_{90}) was corrected by expression of the metallothionein transgene (**Fig. 1**). To explore the possible role of intracellular Ca^{2+} homeostasis in aging and metallothionein-elicited response on cardiomyocyte mechanical function, we evaluated the intracellular Ca^{2+} transients in fura-2-loaded myocytes. Consistent with prolonged TR_{90} in myocytes from aged FVB mice, myocytes from these mice displayed a significantly reduced rate of intracellular Ca^{2+} clearing, which was alleviated by metallothionein. Murine hearts contract at high frequencies. We examined the steady-state peak shortening amplitude under gradually increased stimulating frequency (0.1–5.0 Hz). The results demonstrate that peak shortening (PS) amplitude decreases dramatically with the increased stimulus frequency from 0.1 to 5.0 Hz. The degree of decline in peak shortening amplitude was significantly greater in the aged FVB group compared with young FVB mice, indicating decreased cardiac contractile reserve capacity at higher stress concentration under aging, while the aging-induced decline in peak shortening amplitude at high frequencies was blunted by expression of the metallothionein transgene.

3. Aging-induced changes in oxidative stress and related protein biomarkers in the hearts were attenuated by metallothionein

Enhanced oxidative stress is commonly found with advanced age. Measurement of superoxide production in cardiomyocytes by DHE fluorescence microscopy showed myocytes from aged FVB mice produced significantly higher levels of superoxide as compared with myocytes from young mice, and this effect was attenuated by metallothionein. To investigate the intrinsic cause-consequence link between aging-induced oxidative stress and metallothionein over-expression, we de-

[1]Correspondence: Division of Pharmaceutical Sciences & Center for Cardiovascular Research and Alternative Medicine, University of Wyoming, Laramie, WY 82071-3375, USA. E-mail: jren@uwyo.edu

doi: 10.1096/fj.05–5288fje

0892-6638/06/0020-1024 © FASEB

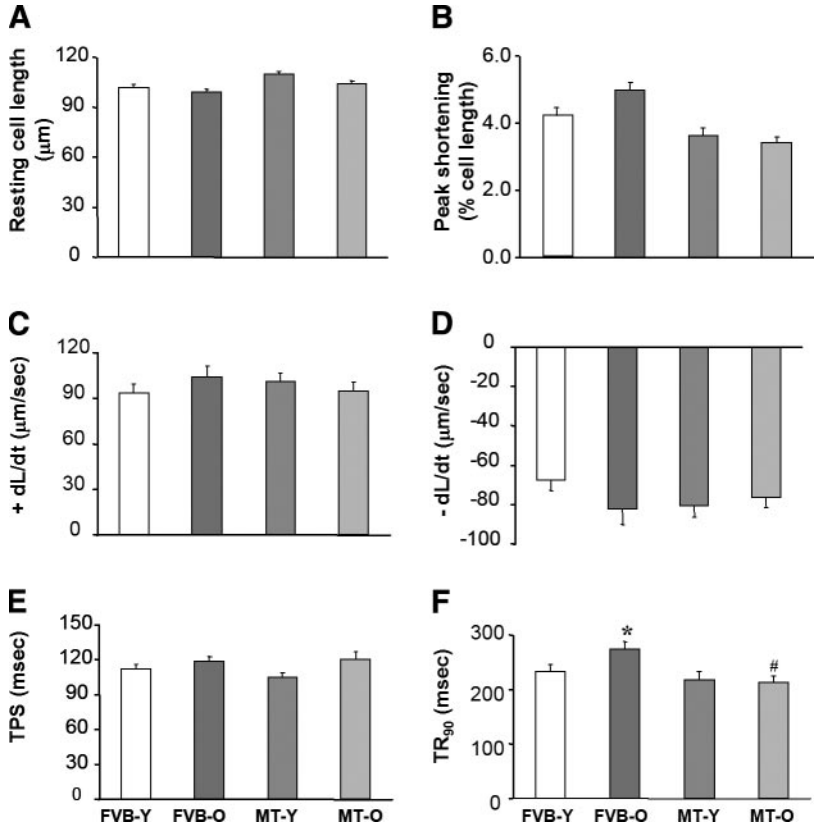

Figure 1. Contractile properties of left ventricular myocytes from young (Y) and aged (O) FVB or metallothionein (MT) mice. *A)* Resting cell length. *B)* Peak shortening (PS, normalized to cell length). *C)* Maximal velocity of shortening ($+dL/dt$). *D)* Maximal velocity of relengthening ($-dL/dt$). *E)* Time-to-peak shortening (TPS). *F)* Time-to-90% relengthening (TR_{90}). Mean ± SE; $n = 140$ cells/group; $^{*}P < 0.05$ vs. FVB-Y group; $^{\#}P < 0.05$ vs. FVB-O group.

tected aconitase activity, NADPH oxidase concentration, active RhoA, cytochrome *c* release using several techniques such as fluorescence, Western blotting, ELISA, and determination of enzyme activity. NADPH oxidase is the most predominant source of superoxide generation, leading to a variety of cardiovascular diseases including diabetes, hypertension, and metabolic syndrome. Similar to its effect on superoxide generation, metallothionein alleviated aging-induced up-regulation of $p47^{phox}$, suggesting a potential antagonistic effect of metallothionein on NADPH oxidase (**Fig. 2**). RhoA, a small GTPase, is well-documented as an inducer of oxidative stress. To explore the role of RhoA in aging-induced oxidative stress, active RhoA was determined by a pull-down assay. Not surprisingly, advanced age initiated an up-regulation of active RhoA, which was inhibited by expression of the metallothionein transgene. We also evaluated mitochondrial cytochrome *c* release as a marker for mitochondrial damage and found enhanced cytosolic cytochrome *c* levels in conjunction with reduced mitochondrial cytochrome *c* levels in aged FVB mouse hearts, indicating enhanced cytochrome *c* release. Nitrotyrosine is a biomarker for protein nitration by peroxynitrite. Evaluation of nitrotyrosine by ELISA indicated that neither aging nor metallothionein transgene expression affected nitrotyrosine formation, suggesting protein nitration is unlikely a major contributor to aging-induced cardiac defects. To further explore aging-induced oxidative stress, we measured cardiac aconitase levels. Aconitase is an iron-sulfur enzyme located in citric acid cycle, and the mitochondrial aconitase activity is closely associated with oxidative stress. Our results showed that aging led to decreased activity of aconitase, consistent with the previous studies, and metallothionein rectified the aging-induced decrease in aconitase activity.

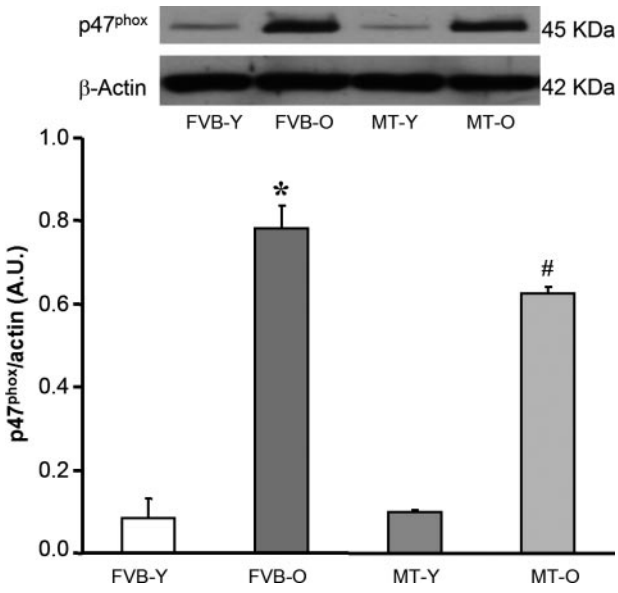

Figure 2. Effect of metallothionein overexpression on $p47^{phox}$ expression in young and aged cardiomyocytes. *Insets)* Representative immunoblots of the NADPH oxidase subunit $p47^{phox}$ and β-actin using specific antibodies. Mean ± SE; $n = 3$; $^{*}P < 0.05$ vs. FVB-Y group; $^{\#}P < 0.05$ vs. FVB-O group.

CONCLUSIONS AND SIGNIFICANCE

Recent data suggested that metallothionein, a low molecular wieght heavy metal chelating antioxidant, exerts protective effects against diabetes- and insulin resistance-induced cardiac damage. However, the impact of metallothionein on cardiac aging and life span has not been elucidated.

Our present study revealed that metallothionein exerts similar effects against the aging process especially cardiac aging. Accumulation of oxygen free radicals or oxidative stress directly compromises ventricular function through NADPH oxidase activity, activation of stress signaling molecules, stimulation of renin-angiotensin system, and direct myogenic effects on heart muscles. Reduction of oxidative stress by either enzymatic or nonenzymatic antioxidants has been shown to improve cardiac function and reduce cardiac apoptosis. In the current study, advanced age elicited oxidative stress without hyperglycemia or hypertension, thus excluding contribution of diabetes and hypertension to our aging model. Data from this study revealed that ventricular myocytes from aged FVB mice displayed prolonged relaxation (TR_{90}), while all other mechanical indices (PS, maximal velocity of shortening/relengthening, time-to-peak shortening) were normal. Moreover, aged cardiomyocytes exhibited diminished stress tolerance manifested as significantly reduced peak shortening at higher stimulating frequencies. These data are consistent with our previous findings using murine model (at similar ages). Reduced intracellular Ca^{2+} clearance rate in aged FVB myocytes is in line with prolonged relaxation duration and reduced intracellular Ca^{2+} cycling ability (reduced PS at high stimulating frequencies) in cardiomyocytes from aged animals.

Given the facts that accumulation of oxygen free radicals or oxidative stress directly compromises ventricular function through NADPH oxidase activity, activation of stress signaling molecules, stimulation of renin-angiotensin system, and direct myogenic effects, our data suggest that metallothionein-elicited antagonism of aging-associated increase in oxidative stress may play a beneficial role against cardiac aging and prolong life span. Mitochondria have been speculated as the major site for oxidative stress-induced damage, although mammalian evidence is sparse. In present study, the aging-induced decrease of mitochondrial aconitase activity was alleviated by metallothionein showed us the possible role of metallothionein transgene. Recent evidence indicates that the small GTPase RhoA participates in the regulation of multiple cell functions, including adhesion, proliferation, migration, and Ca^{2+} homeostasis through kinase cascade activation. The current results indicated that aging-induce active RhoA increase was corrected by metallothionein.

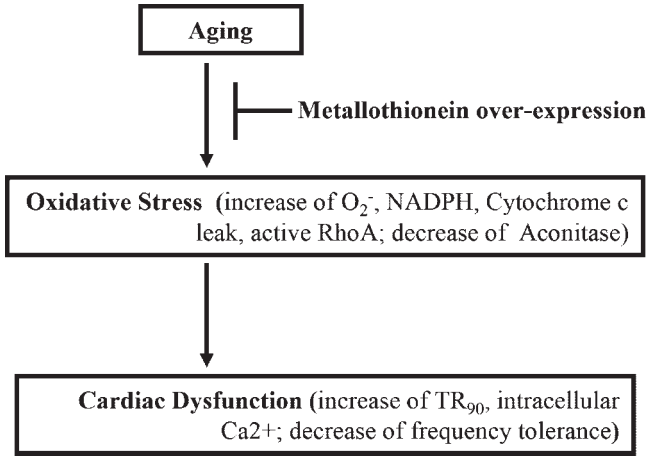

Figure 3. Scheme description of the metallothionein role in prolonged life span. Aging induces the increase of oxidative stress resulting cardiac dysfunctions. Over-expression of metallothionein, a potent free radical scavenger, prolongs the life span, and preserves the cardiac functions via alleviation of oxidative stress.

Collectively, our present data revealed that overexpression of the metallothionein transgene prolonged life span (**Fig. 3**). Furthermore, the metallothionein transgene preserved cardiac contractile functions, improved intracellular Ca^{2+} homeostasis, and restored cardiac contractile capacity under high stimulus frequency, which are cardiac dysfunctions in aged mice. All these function alterations are associated with oxidative stress biomarkers. These results disclose that metallothionein may be beneficial in protecting against aging-induced cardiac dysfunction and oxidative stress and, thus, may prolong life span. FJ

Metallothionein prolongs survival and antagonizes senescence-associated cardiomyocyte diastolic dysfunction: role of oxidative stress

Xiaoping Yang,* Thomas A. Doser,* Cindy X. Fang,* Jennifer M. Nunn,* Rajiv Janardhanan,* Meijun Zhu,† Nair Sreejayan, Mark T. Quinn,‡ and Jun Ren*,[1]

*Division of Pharmaceutical Sciences and Center for Cardiovascular Research and Alternative Medicine, and †Department of Animal Science, University of Wyoming, Laramie, Wyoming, USA; and ‡Department of Veterinary Molecular Biology, Montana State University, Bozeman, Montana, USA

ABSTRACT **Senescence is accompanied by oxidative stress and cardiac dysfunction, although the link between the two remains unclear. This study examined the role of antioxidant metallothionein on cardiomyocyte function, superoxide generation, the oxidative stress biomarker aconitase activity, cytochrome *c* release, and expression of oxidative stress-related proteins, such as the GTPase RhoA and NADPH oxidase protein $p47^{phox}$ in young (5–6 mo) and aged (26–28 mo) FVB wild-type (WT) and cardiac-specific metallothionein transgenic mice. Metallothionein mice showed a longer life span (by ~4 mo) than FVB mice evaluated by the Kaplan-Meier survival curve. Compared with young cardiomyocytes, aged myocytes displayed prolonged TR_{90}, reduced tolerance to high stimulus frequency, and slowed intracellular Ca^{2+} decay, all of which were nullified by metallothionein. Aging increased superoxide generation, active RhoA abundance, cytochrome *c* release, and $p47^{phox}$ expression and suppressed aconitase activity without affecting protein nitrotyrosine formation in the hearts. These aging-induced changes in oxidative stress and related protein biomarkers were attenuated by metallothionein. Aged metallothionein mouse myocytes were more resistant to the superoxide donor pyrogallol-induced superoxide generation and apoptosis. In addition, aging-associated prolongation in TR_{90} was blunted by the Rho kinase inhibitor Y-27632. Collectively, our data demonstrated that metallothionein may alleviate aging-induced cardiac contractile defects and oxidative stress, which may contribute to prolonged life span in metallothionein transgenic mice.—Yang, X., Doser, T. A., Fang, C. X., Nunn, J. M., Janardhanan, R., Zhu, M., Sreejayan, N., Quinn, M. T., Ren, J. Metallothionein prolongs survival and antagonizes senescence-associated cardiomyocyte diastolic dysfunction: role of oxidative stress *FASEB J.* 20, E260–E270 (2006)**

Key Words: contraction · oxidative stress · antioxidant · longevity

THE PREVALENCE OF HEART FAILURE is significantly higher in the elderly compared with the middle-aged or young population, indicating that aging or senescence *per se* plays an important role in cardiac dysfunction (1). Ample evidence has implicated free radical accumulation or oxidative stress as an essential culprit player in aging-related cardiovascular dysfunction (2–6). The "free radical theory of aging," first postulated by Harman (7), has been perhaps the most widely accepted hypothesis for the biology of aging. According to this theory, the progressively accumulated oxidant insult with increased age is responsible for enhanced oxidative stress *en route* to ultimate biological events of senescence (7). The free radical theory of aging has paved its way to the modern concept of "mitochondrial theory of aging," which credits mitochondria as the main culprits for oxidative stress (8). Aging-related accumulation of free radicals or oxidative stress has been demonstrated to be responsible for senescent organ damage including hearts (9–11). However, the precise mechanisms of action underlying aging-induced cardiac contractile dysfunction remain poorly understood. Recent data suggested that metallothionein, a low molecular weight heavy metal chelating antioxidant, exerts protective effects against diabetes- and insulin resistance-induced cardiac damage (12–14). However, the impact of metallothionein on cardiac aging and life span has not been elucidated. The aim of this investigation was to examine the effect of cardiac-specific over-expression of metallothionein on life span, cardiac aging, and oxidative stress. Our results revealed that expression of the metallothionein transgene prolonged life span, preserved cardiac contractile functions, improved intracellular Ca^{2+} homeostasis, restored cardiac contractile capacity under high stimulus frequency in advanced age, and alleviated aging-associated elevation in biomarkers of oxidative stress and cell death. These data suggest that metallothion-

[1] Correspondence: Division of Pharmaceutical Sciences & Center for Cardiovascular Research and Alternative Medicine, University of Wyoming, Laramie, WY 82071-3375, USA. E-mail: jren@uwyo.edu

doi: 10.1096/fj.05-5288fje

0892-6638/06/0020-0260 © FASEB

ein-elicited antagonism of aging-associated increase in oxidative stress may play a beneficial role against cardiac aging and prolong life span.

MATERIALS AND METHODS

Experimental animals and Kaplan-Meier's survival curve

The experimental procedure was approved by the Institutional Animal Use and Care Committee at the University of Wyoming (Laramie, WY). All animal procedures were in accordance with the National Institute of Health animal care standards. Production and characterization of metallothionein transgenic mice were described in detail previously (14). In brief, a 11.4 kb metallothionein cDNA construct driven by α-myosin heavy chain (α-MHC) promoter containing entire coding sequences of the human metallothionein-IIa gene was purified on a matrix of diatemaceous earth (Prepagene; Bio-Rad Laboratories, Richmond, CA) and filtered through a 0.22 μm filter. Approximately 100 copies of the purified transgene insert were microinjected into one pronucleus of each one-cell mouse embryo of the inbred strain FVB. Twenty microinjected embryos were implanted into each pseudopregnant female, which was allowed to come to term. For identification of the transgenic founder mice, genomic DNA isolated from 4-wk-old mice (by tail clips) was subjected to Southern and dot blot analyses was probed with an 850-bp *Nco*I/*Bgl*II fragment derived from the human metallothionein-IIa gene. This probe was hybridized with an 11.5-bp *Sac*I fragment of the genomic DNA digests, consistent with the presence of a unique *Sac*I site in the MHC-driven metallothionein-IIa transgene. Founder mice were cross-bred, and offspring were identified by PCR using a primer pair derived from the MHC promoter and human metallothionein-IIa gene. Male positive transgenic mice (heterozygotes with a 5- to 10-fold increase in metallothionein expression) and negative littermates were used for our current study at either 5–6 mo of age (denoted as "young") or 26–28 mo of age (denotes as "aged"). Mice were maintained with a 12/12-light/dark cycle with free access to tap water. The fur color was used as a marker for metallothionein (dark brown) or WT FVB (white) mouse identification (13). To configure the Kaplan-Meier survival curve, male FVB and metallothionein mice were separated after weaning (<12 mice per cage). Mice were checked weekly, and mortality was recorded every 2 months.

Cell isolation procedures

Mouse hearts were removed under anesthesia (150 mg/kg ketamine and 22.5 mg/kg xylazine, ip) and were perfused with Krebs-Henseleit bicarbonate buffer containing (in mM): 118 NaCl, 4.7 KCl, 1.2 $MgSO_4$, 1.2 KH_2PO_4, 25 $NaHCO_3$, 10 HEPES, 11.1 glucose (Glc), and 10 butanedione with 5% CO_2-95% O_2. Hearts were subsequently digested with 223 U/ml collagenase D (Boehringer Mannheim, Indianapolis, IN) for 10 min at 37°C. After perfusion, left ventricles were removed and minced. Extracellular Ca^{2+} was incrementally added back to 1.25 mM. Cell viability was ~70% in all four animal groups. Functional studies were conducted between 1 and 8 h of isolation and myocytes with obvious sarcolemmal blebs or spontaneous contractions were not used for study (15). To evaluate the involvement of RhoA in aging-associated alteration in mechanical function, a cohort of myocytes from young and aged FVB mice was incubated with the Rho kinase inhibitor Y-27632 (10 μM) for 4 h in a defined medium consisting of Medium 199 with Earle's salts containing HEPES (25 mM) and $NaHCO_3$ (25 mM), supplemented with albumin (2 mg/ml), L-carnitine (2 mM), creatine (5 mM), taurine (5 mM), insulin (100 nM), penicillin (100 U/ml), streptomycin (100 μg/ml), and gentamicin (5 μg/ml) at 37°C.

Cell shortening/relengthening

Mechanical properties of ventricular myocytes were assessed using a SoftEdge MyoCam system (IonOptix Corporation, Milton, MA) (15). In brief, left ventricular myocytes were placed in a chamber mounted on the stage of an inverted microscope (Olympus, IX-70) and superfused at 25°C with a buffer containing (in mM): 131 NaCl, 4 KCl, 1 $CaCl_2$, 1 $MgCl_2$, 10 Glc, and 10 HEPES, at pH 7.4. The cells were field stimulated with suprathreshold voltage at a frequency of 0.5 Hz (unless otherwise stated), 3 msec duration, using a pair of platinum wires placed on opposite sides of the chamber connected to a FHC stimulator (Brunswick, NE). The myocyte being studied was displayed on a computer monitor using an IonOptix MyoCam camera. An IonOptix SoftEdge software was used to capture changes in cell length during shortening and relengthening. Cell shortening and relengthening were assessed using the following indices: peak shortening (PS), the amplitude myocytes shortened on electrical stimulation, an indicative of peak ventricular contractility; time-to-PS (TPS), the duration of myocyte shortening, an indicative of systolic duration; time-to-90% relengthening (TR_{90}), the duration to reach 90% relengthening, an indicative of diastolic duration (90% rather 100% relengthening was used to avoid noisy signal at baseline concentration); and maximal velocities of shortening/relengthening, maximal slope (derivative) of shortening and relengthening phases, indicative of maximal velocities of ventricular pressure increase/decrease. In the case of altering stimulus frequency, the steady-state contraction of myocyte was achieved (usually after the first 5–6 beats) before PS amplitude was recorded (1).

Intracellular Ca^{2+} transient measurement

Intracellular Ca^{2+} was measured using a dual-excitation, single-emission photomultiplier system (IonOptix) in myocytes loaded with fura-2-acetoxymethyl ester (0.5 μM) (15). Myocytes were placed on an inverted microscope and imaged through an Olympus (model: IX-70) Fluor × 40 oil objective. Myocytes were exposed to light emitted by a 75-W halogen lamp through either a 360- or 380-nm filter while being stimulated to contract at 0.5 Hz. Fluorescence emissions were detected between 480 and 520 nm by a photomultiplier tube after initial illumination at 360 nm for 0.5 s and then at 380 nm for the duration of the recording protocol. The 360-nm excitation reading was repeated at the end of the protocol. Qualitative evaluation of intracellular Ca^{2+} was inferred from fura-2 fluorescence intensity (FFI) changes (ΔFFI). A Chebyshev equation was used to evaluate the intracellular Ca^{2+} decay constant. Myocyte shortening was also evaluated in a cohort of the fura-2-loaded ventricular myocytes simultaneously to compare their temporal relationship with the fluorescence signal. However, their mechanical properties were not used for data summary due to the apparent Ca^{2+} buffering effect of fura-2.

Intracellular fluorescence measurement of superoxide

Intracellular superoxide concentration was monitored by changes in fluorescence intensity resulting from intracellular probe oxidation, as described previously (16). Freshly isolated cardiac myocytes were loaded with 2.5 μM dihydroethidium (DHE, Molecular Probes, Eugene, OR) for 15 min at 37°C, washed with PBS buffer, and loaded into coverslips. Cells were sampled randomly using an Olympus BX- 51 microscope equipped with a MagnaFir SP digital camera and ImagePro

image analysis software (Media Cybernetics, Silver Spring, MD). All test conditions were kept identical. The grid crossing method was employed for cell selection in more than 15 visual fields per cell group. To evaluate the effect of metallothionein on resistance to superoxide generation, cardiomyocytes from aged FVB and metallothionein mice were incubated with pyrogallol (100 μM), a superoxide generator (17), for 2 h before superoxide generation was determined.

Mitochondrial cytochrome *c* release

Ventricles were minced and homogenized by Polytron in ice-cold MSE buffer [220 mM mannitol, 70 mM sucrose, 2 mM ethylene glycol-bis(aminoethylether)-tetraacetic acid (EGTA), 5 mM 3-(4-morpholino) propane sulfonic acid (MOPS), pH 7.4, 0.2% BSA and a protease inhibitor cocktail containing 4-(2-aminoethyl) benzenesulfonyl fluoride (AEBSF), E-64, bestatin, leupeptin, aprotinin, and sodium ethylenediaminetetraacetic acid (EDTA) (Sigma, St. Louis, MO)]. The homogenates were centrifuged for 10 min at 600 *g* to remove unbroken tissue and nuclei, and the supernatants were centrifuged for 10 min at 3000 *g* to pellet mitochondria. The supernatants were further centrifuged for 1 h at 16,000 *g* at 4°C to obtain cytosol. The mitochondrial pellet was dissolved in radio-immuno-precipitation assay (RIPA) lysis buffer containing 150 mM NaCl, 0.25 deoxycholic acid, 1% Nonidet P-40, 1 mM EDTA, 50 mM Tris-HCl, pH 7.4 (Upstate, Lake Placid, NY), and 1% protease inhibitor cocktail and centrifuged at 10,000 *g* for 30 min at 4°C to make a soluble protein. Supernatants were collected and protein concentrations were determined by Micro bicinchoninic acid (BCA) protein assay kit (Pierce Chemical, Rockford, IL). Proteins were boiled in Laemmli sample buffer (Bio-Rad Laboratories, Hercules, CA); 50 μg protein of mitochondrial fraction or cytosol were separated by 15% sodium dodecyl sulfate PAGE (SDS-PAGE) in a Mini-PROTEAN II minigel apparatus (Bio-Rad Laboratories, Hercules, CA) and electrophoretically transferred to a nitrocellulose membrane. The membranes were incubated for 1 h at room temperature in blocking buffer (5% w/v non fat dry milk in tris buffered saline containing 0.1% Tween 20, TBS-T). Membranes were incubated in anti-rabbit cytochrome *c* polyclonal antibody (pAb) 1:1000 followed by incubation with horseradish peroxidase-coupled anti-rabbit secondary antibody (Ab; Cell Signaling Technology, Beverly, MA). Immunoreactive bands were visualized using enhanced chemiluminescence reagents (Cell Signaling Technology). After immunoblotting, the film was scanned and the intensity of immunoblot bands was detected with a GS-800 Calibrated Densitometer (Bio-Rad Laboratories, Hercules, CA). Blots for cytosol were stripped and reprobed with Ab directed monoclonal antimouse β-actin, which serves as an internal loading control (Cell Signaling Technology) (18).

Nitrotyrosine determination

Myocardial tissue was homogenized in RIPA lysis buffer with 1% protease inhibitor cocktail using a PRO 200 homogenizer followed by sonication with a dismembrator (Fisher Scientific, Pittsburgh, PA). Homogenates were centrifuged for 10 min at 12,500 *g* at 4°C. Supernatants were collected, and lysates containing 100 μg protein were applied to disposable sterile microtiter plates (Corning Glassworks, Corning, NY) and incubated overnight at 4°C. The plate was then washed twice with 200 μl of TBS-T followed by incubation with heat-inactivated 200 μl 1% BSA in TBS for 1 h at 37°C to block nonspecific binding. After being washed three times with TBS-T, rabbit pAb against nitrotyrosine (Cell Signaling Technology; 1:2000 dilution) was added to incubate for 1 h at 37°C followed by addition of secondary Ab (horseradish peroxidase-conjugated anti-rabbit IgG, 1:2000 dilution) for 1 h at 37°C. After being washed five times with TBS-T, the peroxidase reaction product was generated using 100 μl TMB (Abbott Diagnostics, Abbott Park, IL). Plates were incubated for 20 min in the dark at room temperature, and the reaction was stopped by addition of 0.3 N HCl to each well. Optical density was measured at 450 nM with a SpectraMax 190 Microplate Spectrophotometer (Molecular Devices, Sunnyvale, CA; ref 18).

Western blot analysis of metallothionein and NADPH oxidase $p47^{phox}$ subunits

Western blot analysis of metallothionein and NADPH oxidase subunit was performed on total protein lysate prepared from procedure as described above. Briefly, protein samples were separated on 10% SDS-polyacrylamide gels in a minigel apparatus and transferred to nitrocellulose membranes. Membranes were probed with antimouse metallothionein, antimouse $p47^{phox}$, and anti-β-actin antibodies (19,20) followed by incubation with horseradish peroxidase-coupled antimouse secondary Ab (Cell Signaling Technology). Metallothionein Ab was purchased from Santa Cruz Biotechnology (Santa Cruz Biotechnology, Santa Cruz, CA). After immunoblotting, the film was scanned and intensity of immunoblot bands was detected with a Bio-Rad calibrated densitometer (21). β-actin was used as an internal loading control. The monoclonal β-actin Ab was obtained from Cell Signaling Technology.

Aconitase activity

Mitochondrial fractions prepared from whole heart homogenate were resuspended in 0.2 mM sodium citrate. After determination of protein concentration using the bicinchoninic acid (BCA) protein assay kit and BSA as a standard, aconitase activity assay (Aconitase activity assay kit, Aconitase-340 assay, OxisResearch, Portland, OR) was performed according to manufacturer instructions with minor modifications. Briefly, mitochondrial sample (50 μl) was mixed in a 96-well plate with 50 μl trisodium citrate (substrate) in Tri-HCl pH 7.4, 50 μl isocitrate dehydrogenase (enzyme) in Tris-HCl, and 50 μl NADP in Tris-HCl. After being incubated for 15 min at 37°C with 50 rpm shaking (I2400 Incubator Shaker, New Brunswick Scientific, Edison, NJ), the absorbance was dynamically recorded at 340 nm every minute for 5 min with a SpectraMax 190 Microplate Spectrophotometer. During the assay, citrate is isomerized by aconitase into isocitrate and eventually α-ketoglutarate. The Aconitase-340 assay measures NADPH formation, a product of the oxidation of isocitrate to α-ketoglutarate. Tris-HCl buffer (pH 7.4) was served as blank (22).

Determination of active RhoA

RhoA expression was measured according to the EZ-Detect Rho activity kit instructions (Pierce Chemical, Rockford, IL). Briefly, heart lysates known concentrations were pull-down in spin cup by adding of SwellGel Immobilized Gluthione Disc and glutathione S-transferase-Rhotekin-RBD. After incubation for 1 h at 4°C, the resin containing active Rho was carefully washed three times with wash buffer (provided by the supplier). The protein was recovered from resin by denaturing the resin. Regular Western blot was run as described as above, using 12% SDS-PAGE as separate gel. The nitrocellulose membrane was blocked in 3% BSA at room temperature for 2 h and incubated with 1:500 diluted anti-Rho primary Ab, followed by HRP-conjugated goat antimouse IgG secondary Ab (23). For the total RhoA, conventional Western blot was directly performed with heart lysates to

detect total RhoA concentration. Equal loading was confirmed by both protein concentration assay and β-actin.

Determination of apoptosis

To assess the effect of metallothionein on aging-induced apoptosis, cardiomyocytes from aged FVB and metallothionein mice were incubated with pyrogallol (100 μM), a superoxide donor and a reactive oxygen species (ROS) inducer (17), for 2 h before levels of cleaved caspase-9 was determined using Western blot analysis. Cleaved caspase-3 is a key biomarker of apoptosis (24). After pyrogallol treatment, the cardiomyocytes were collected by centrifugation at 300 rpm for 5 min. The cells were lysed and Western blot was performed as described (19). The membrane was probed with caspase-9 Ab (Cell Signaling Technology, 1:1000 dilution).

Statistical analyses

Data are presented as mean ± SE. Log rank test was used for Kaplan-Meier survival curve (25). Statistical significance ($P<0.05$) for all other variables was determined by ANOVA followed by a Dunnett's *post hoc* analysis.

RESULTS

General features of young and aged FVB or metallothionein mice

There were no differences in body, heart, liver, and kidney weights as well as organ size (normalized to body wt) between age-matched FVB and metallothionein over-expressing mice. The body and organ weights were significantly heavier in aged mice compared with younger ones, as expected. However, organ size of heart, liver, and kidney were similar between young and aged mice (**Table 1**). There was no difference in fasting Glc or blood pressure levels among the four mouse groups, excluding the presence of diabetes or hypertension (data not shown). Western blot analysis revealed that cardiac expression of metallothionein in young metallothionein transgenic mice was ~5-fold higher than that of young FVB mice. While aging itself did not affect metallothionein expression in FVB mice, the metallothionein expression in aged metallothionein mice was enhanced even further (~7-fold higher than aged FVB; **Fig. 1*A***). The Kaplan-Meier survival curve shows that metallothionein transgenic mice display a ~4 mo longer life span compared with FVB mice (Fig. 1*B*). The average life span was 30.14 ± 1.76 and 26.49 ± 1.75 mo in metallothionein and FVB groups, respectively ($P<0.05$ between the two groups using the log rank test). The two curves start to separate from each other after 20 mo of age with metallothionein mice exhibiting a reduced mortality rate.

Baseline mechanical and intracellular Ca^{2+} properties of left ventricular myocytes

Data shown in **Fig. 2** indicate that time-to-90% relengthening (TR_{90}) was significantly prolonged in the aged FVB mouse group, while all other mechanical indices remain unchanged compared with young FVB group. Such aging-triggered diastolic dysfunction is consistent with our previous report (1). Interestingly, the aging-induced prolongation of TR_{90} was corrected by expression of the metallothionein transgene. To explore the possible role of intracellular Ca^{2+} homeostasis in aging and metallothionein-elicited response on cardiomyocyte mechanical function, we evaluated the intracellular Ca^{2+} transients in fura-2 loaded myocytes. Our result indicated similar resting FFI and ΔFFI in myocytes from young and aged FVB groups. Consistent with prolonged TR_{90} in myocytes from aged FVB mice, myocytes from these mice displayed a significantly reduced rate of intracellular Ca^{2+} clearing, which was alleviated by metallothionein (**Fig. 3**). Lastly, metallothionein expression itself did not affect the mechanical or intracellular Ca^{2+} properties in young mice, indicating that the antioxidant does not innately influence intrinsic cardiomyocyte contractile function.

Effect of increasing stimulation frequency on myocyte shortening

Murine hearts contract at high frequencies. We examined the steady-state PS amplitude under gradually increased stimulating frequency (0.1–5.0 Hz). All recordings were normalized to PS obtained at 0.1 Hz for the same cardiomyocyte. The results demonstrate that PS amplitude decreases dramatically with increased stimulus frequency from 0.1 Hz to 5.0 Hz (**Fig. 4*A***). The degree of decline in PS amplitude was significantly greater in the aged FVB group compared with young FVB mice, indicating decreased cardiac contractile

TABLE 1. *General characteristics of young and aged FVB and metallothionein (MT) transgenic mice*

Mouse group	FVB-young (n=16)	FVB-aged (n=16)	MT-young (n=16)	MT-aged (n=16)
Body weight (g)	20.5 ± 0.6	30.9 ± 0.8*	19.2 ± 0.8	31.0 ± 0.7*
Heart weight (mg)	131 ± 10	194 ± 14*	120 ± 10	179 ± 14*
Heart/weight (mg/g)	6.30 ± 0.39	6.36 ± 0.51	6.27 ± 0.42	5.72 ± 0.38
Liver weight (mg)	1161 ± 58	1674 ± 70*	1067 ± 41	1604 ± 96*
Liver/body weight (mg/g)	56.4 ± 2.0	54.3 ± 2.0	56.5 ± 2.2	51.2 ± 2.4
Kidney weight (mg)	281 ± 11	453 ± 26*	273 ± 22	478 ± 21*
Kidney/body weight (mg/g)	13.66 ± 0.31	14.66 ± 0.72	14.03 ± 0.76	15.40 ± 0.59

Mean ± SE, n = number of mice per group, *$P < 0.05$ *vs.* young group of the same line.

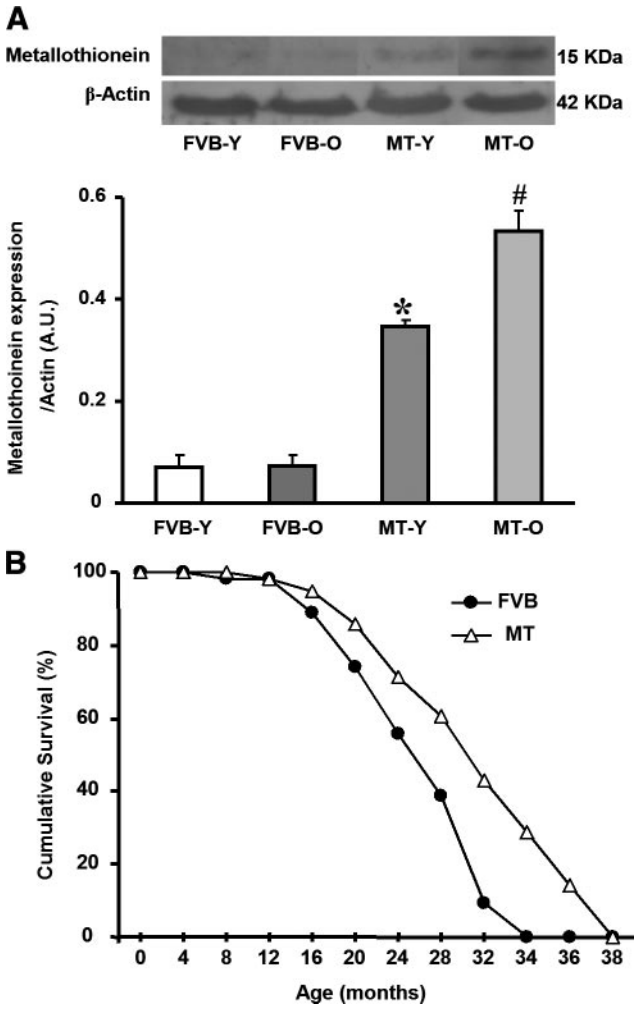

Figure 1. *A)* Metallothionein expression in hearts of young (Y) and aged (O) FVB or metallothionein (MT) mice. *Insets)* Representative immunoblots of metallothionein and β-actin using specific antibodies. Mean ± SE; $n = 3$; $^{*}P < 0.05$ vs. FVB-Y group, $^{\#}P < 0.05$ vs. all other groups. *B)* Cumulative survival curves (Kaplan-Meier survival analysis) of male FVB and MT mice. Death of mice was checked weekly and reported every 4 months in the first 32 months and then every 2 months. Cumulative survival rate was plotted against the time course (n=55–56 mice/group). Life span was 26.49 ± 1.75 vs. 30.14 ± 1.76 monaths in FVB and MT mice, respectively. Mean ± SE; $P <$ 0.05 between 2 groups evaluated by log rank test.

reserve capacity at higher stress concentration under aging, as reported previously (1). Interestingly, the aging-induced decline in peak shortening amplitude at high frequencies was blunted by expression of the metallothionein transgene. Metallothionein itself did not elicit any significant effect on stimulus frequency-PS relationship in myocytes from young mice. Lastly, changes in the stimulus frequency from 0.1 Hz to 5.0 Hz did not significantly affect the diastolic resting cell length (Fig. 4*B*)

Intracellular superoxide levels and NADPH oxidase expression

Measurement of superoxide production in cardiomyocytes by DHE fluorescence microscopy (12,16,26) showed myocytes from aged FVB mice produced significantly higher levels of superoxide as compared with myocytes from young mice, and this effect was significantly attenuated by metallothionein (**Fig. 5**). NADPH oxidase is the most predominant source of superoxide generation, leading to a variety of cardiovascular diseases including diabetes, hypertension and metabolic syndrome (1, 27). Our data revealed significantly up-regulated $p47^{phox}$ subunit of the NADPH oxidase in aged FVB hearts compared with the young FVB group (**Fig. 6**), consistent with elevated superoxide levels in the same mice. Similar to its effect on superoxide generation, metallothionein alleviated aging-induced up-regulation of $p47^{phox}$, suggesting a potential antagonistic effect of metallothionein on NADPH oxidase. These results suggest that NADPH oxidase is likely responsible for aging-induced elevation in superoxide levels and further confirmed the notion of metallothionein as a free radical scavenger (12–14, 28, 29).

Effect of metallothionein on aging-induced increases of RhoA and cytochrome *c release*

Enhanced oxidative stress is often found in advanced age *en route* to irreversible damage of proteins or lipids (22). However, proteins responsible for enhanced oxidative stress have not been carefully identified. RhoA, a small GTPase, is well-documented as an inducer of oxidative stress (30–33). To explore the role of RhoA in aging-induced oxidative stress, active RhoA was determined by a pull-down assay. Not surprisingly, advanced age initiated an up-regulation of active RhoA, which was inhibited by expression of the metallothionein transgene, but there is not a significant difference in total RhoA expression among the four animal groups examined (**Fig. 7**). We also evaluated mitochondrial cytochrome *c* release as a marker for mitochondrial damage (12,18) and found enhanced cytosolic cytochrome *c* levels in conjunction with reduced mitochondrial cytochrome *c* levels in aged FVB mouse hearts, indicating enhanced cytochrome *c* release (**Fig. 8**). Similar to its effect on RhoA, metallothionein ablated aging-induced enhanced release of cytochrome *c* (Fig. 8).

Nitrotyrosine formation and aconitase activity in FVB and metallothionein mice

Nitrotyrosine is a biomarker for protein nitration by peroxynitrite (12, 18, 34). Evaluation of nitrotyrosine by ELISA indicated that neither aging nor metallothionein transgene expression affected nitrotyrosine formation, suggesting protein nitration is unlikely a major contributor to aging-induced cardiac defects (**Fig. 9**). To further explore aging-induced oxidative stress, we measured cardiac aconitase levels. Aconitase is an iron-sulfur enzyme located in citric acid cycle, and the mitochondrial aconitase activity is closely associated with oxidative stress (22, 35, 36). For example, mitochondrial aconitase is readily damaged by oxidative

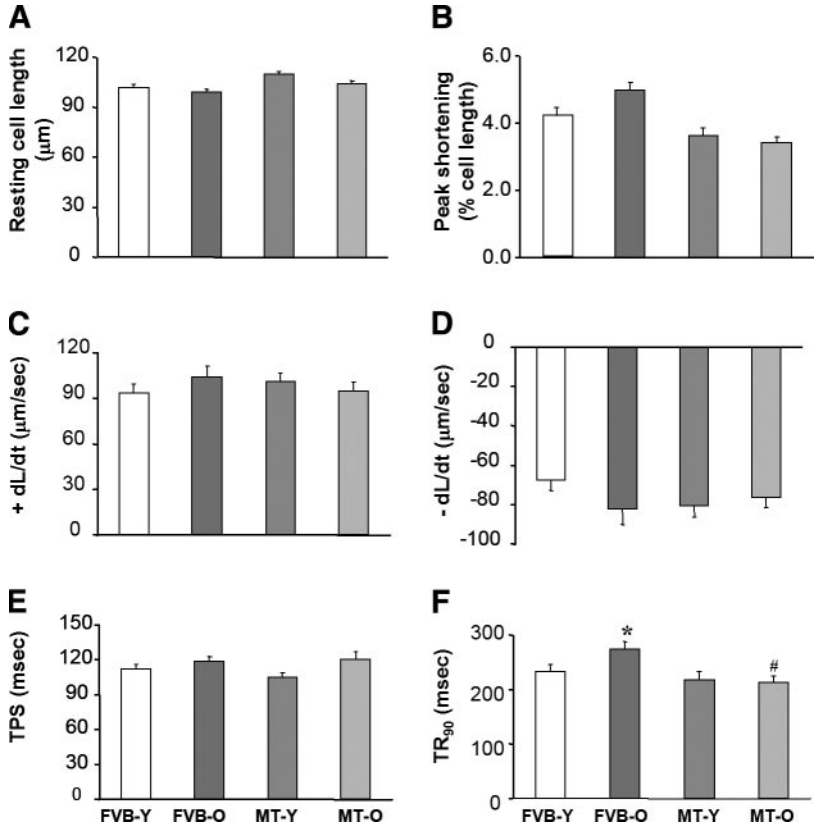

Figure 2. Contractile properties of left ventricular myocytes from young and aged FVB or metallothionein mice. *A)* Resting cell length. *B)* PS (normalized to cell length). *C)* Maximal velocity of shortening ($+dL/dt$). *D)* Maximal velocity of relengthening ($-dL/dt$). *E)* Time-to-peak shortening (TPS). *F)* Time-to-90% relengthening (TR_{90}). Mean ± SE; $n = 140$ cells/group; $^{*}P < 0.05$ vs. FVB-Y group; $^{\#}P < 0.05$ vs. FVB-O group.

stress via removal of an iron from [4Fe-4S] cluster (37). Our results showed that aging led to decreased activity of aconitase, consistent with the previous studies (22, 36). Interestingly, metallothionein rectified the aging-induced decrease in aconitase activity (Fig. 9).

Sensitivity to pyrogallol-elicited apoptosis and superoxide generation in aged FVB and metallothionein mouse myocytes

To determine the effect of metallothionein on sensitivity of cardiomyocytes to ROS-induced apoptosis and superoxide generation, the superoxide generator pyrogallol (100 μM) was used to induce superoxide generation and apoptosis (17). Data displayed in **Fig. 10** indicated that levels of cleaved caspase-9, an important indicator for apoptosis (24) and superoxide, were both significantly lower in aged metallothionein myocytes compared with aged FVB myocytes. These observations were consistent with reduced levels of $p47^{phox}$ (Fig. 6), active RhoA (Fig. 7), and cytosolic cytochrome *c* (Fig. 8) as well as higher aconitase activity (Fig. 9) in aged metallothionein group compared with aged FVB group. More interestingly, pyrogallol-induced signifi-

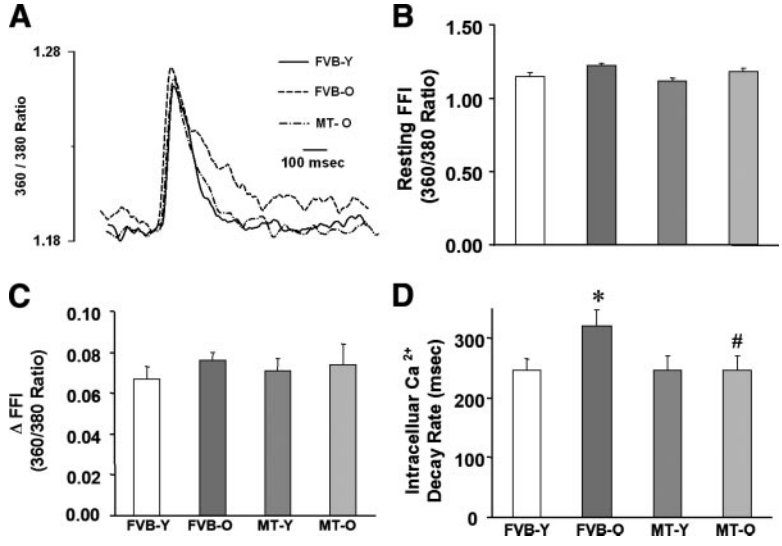

Figure 3. Intracellular Ca^{2+} transient properties of left ventricular myocytes from young and aged FVB or metallothionein mice. *A)* Representative intracellular Ca^{2+} transient traces from FVB-Y, FVB-O and MT-O groups. *B)* Resting fura-2 fluorescence intensity (FFI). *C)* fura-fluorescence intensity change (ΔFFI) in response to electrical stimuli; and (*D*) intracellular Ca^{2+} transient decay rate. Mean ± SE; $n = 53$ cells/group; $^{*}P < 0.05$ vs. FVB-Y group; $^{\#}P < 0.05$ vs. FVB-O group.

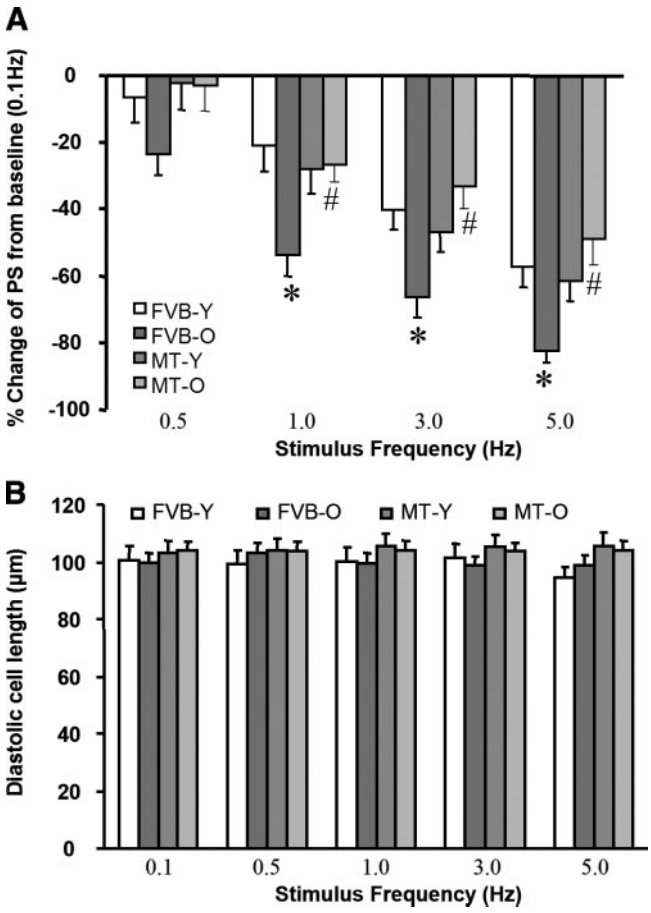

Figure 4. Peak shortening amplitude (*A*) and diastolic resting cell length (*B*) of ventricular myocytes from young and aged FVB or metallothionein mice recorded at different stimulus frequencies (0.1 0.5, 1.0, 3.0, and 5.0 Hz). PS at each stimulus frequency was normalized to that of 0.1 Hz from the same cell. Mean ± SE; $n = 22\sim28$ cells/group; $^{*}P < 0.05$ vs. FVB-Y group; $^{\#}P < 0.05$ vs. FVB-O group.

cant increase in apoptosis and superoxide generation in aged FVB myocytes was either blunted (caspase-9) or significantly attenuated (superoxide generation) in aged metallothionein group, indicating overt resistance to pyrogallol-triggered myocyte superoxide generation and apoptosis by the metallothionein transgene.

Effect of Rho kinase inhibitor Y-27632 on cell shortening in young and aged FVB myocytes

To examine the role of RhoA and Rho kinase signaling in aging-associated cardiomyocyte contractile dysfunction, young and old FVB murine cardiomyocytes were incubated with the Rho kinase inhibitor Y-27632 (10 μM) for 4 h before mechanical function was evaluated (38). As shown in **Fig. 11**, Y-27632 did not affect resting cell length in young or aged FVB groups. PS, ± d*L*/d*t*, and TPS were not affected by either aging or Y-27632. Interestingly, aging-induced prolongation in TR_{90} was blunted by coincubation of Y-27632. Y-27632 itself did not affect any cell mechanics in young FVB myocytes.

DISCUSSION

The major findings of our study are that aging elicits cardiac contractile and intracellular Ca^{2+} dysfunction. Furthermore, aging-induced cardiac contractile and intracellular Ca^{2+} dysfunction was causally associated with enhanced superoxide generation, $p47^{phox}$ expression, RhoA activity, and mitochondrial cytochrome *c* release. Interestingly, these aging-associated alterations in contractile function (at both low and high stimulating frequencies) and oxidative stress signaling were significantly attenuated or abolished by cardiac overexpression of metallothionein. Consistent with the enhanced RhoA activity in aged cardiomyocytes, the aging-induced cardiomyocyte dysfunction was ablated by the Rho kinase inhibitor Y-27632. Metallothionein

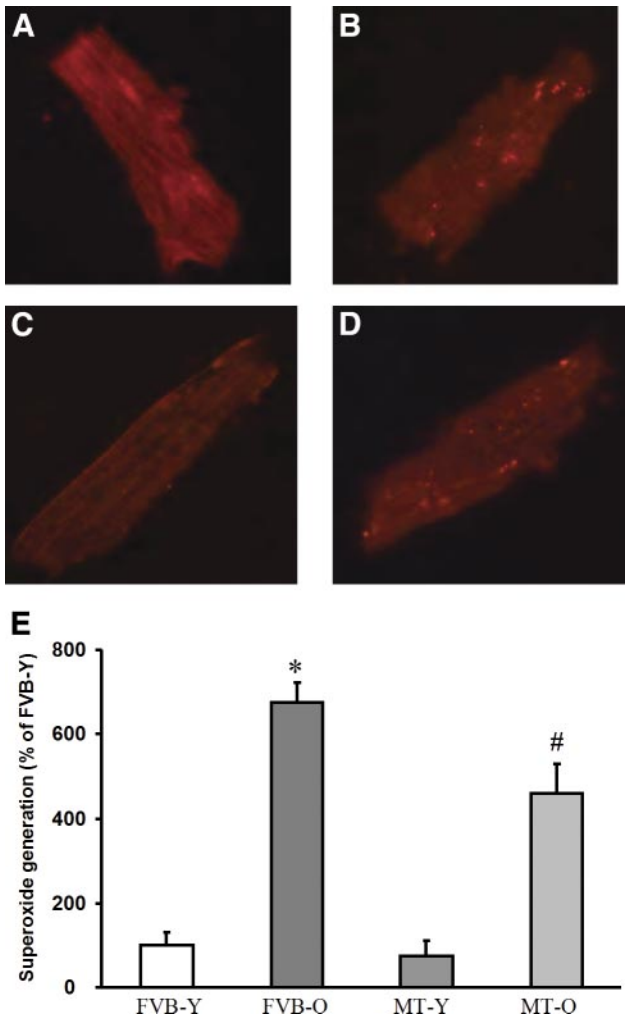

Figure 5. Superoxide (O_2^-) production measured by dihydroethidium (DHE) fluorescence probe. Freshly isolated cardiomyocytes were incubated with 2.5 μM DHE for 15 min before fluorescence microscopy. Bright spots represent the reaction of superoxide with DHE. *A–D* display representative fluorescence images of single cardiomyocytes from FVB-Y (*A*), FVB-O (*B*), MT-Y (*C*), and MT-O (*D*) group. *E* exhibits summarized data normalized to FVB-Y group. Mean ± SE; $n = 123\sim160$ cells/group; $^{*}P < 0.05$ vs. FVB-Y group; $^{\#}P < 0.05$ vs. FVB-O group.

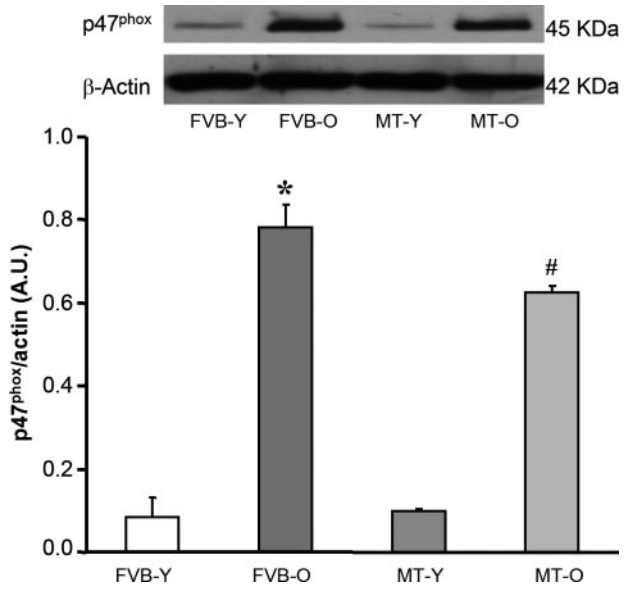

Figure 6. Effect of metallothionein overexpression on p47^{phox} expression at young and aged cardiomyocytes. *Insets*) Representative immunoblots of the NADPH oxidase subunit p47^{phox} and β-actin using specific antibodies. Mean ± SE; $n = 3$; $^{*}P < 0.05$ vs. FVB-Y group, $^{\#}P < 0.05$ vs. FVB-O group.

transgenic mice show a significant resistance to pyrogallol-elicited superoxide generation and apoptosis. Importantly, attenuation of these age-related effects was associated with prolonged life span in metallothionein transgenic mice. Although aging itself does not cause any reduction in cardiac metallothionein levels, our results indicate that metallothionein may be beneficial in protecting against aging-induced cardiac dysfunction, and oxidative stress and, thus, may prolong life span.

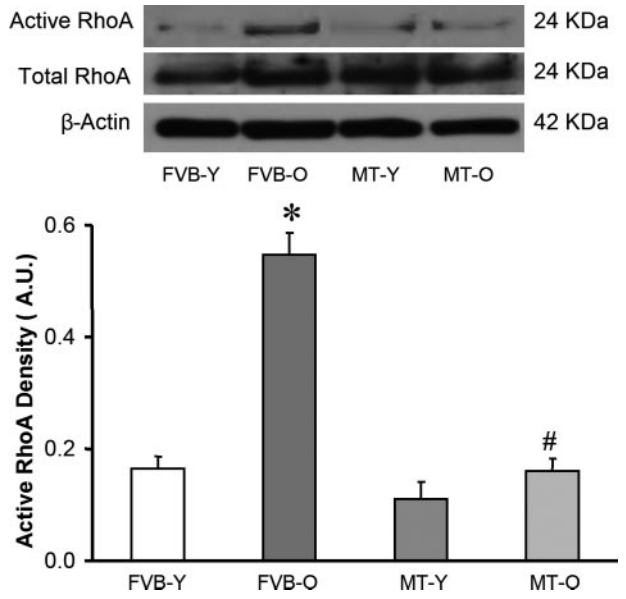

Figure 7. Effect of metallothionein (MT) overexpression on total and active RhoA levels in young and aged cardiomyocytes. *Insets*) Representative immunoblots of RhoA expression in total lysats and pull-down lysates as well as β-actin. Mean ± SE; $n = 3$; $^{*}P < 0.05$ vs. FVB-Y group, $^{\#}P < 0.05$ vs. FVB-O group.

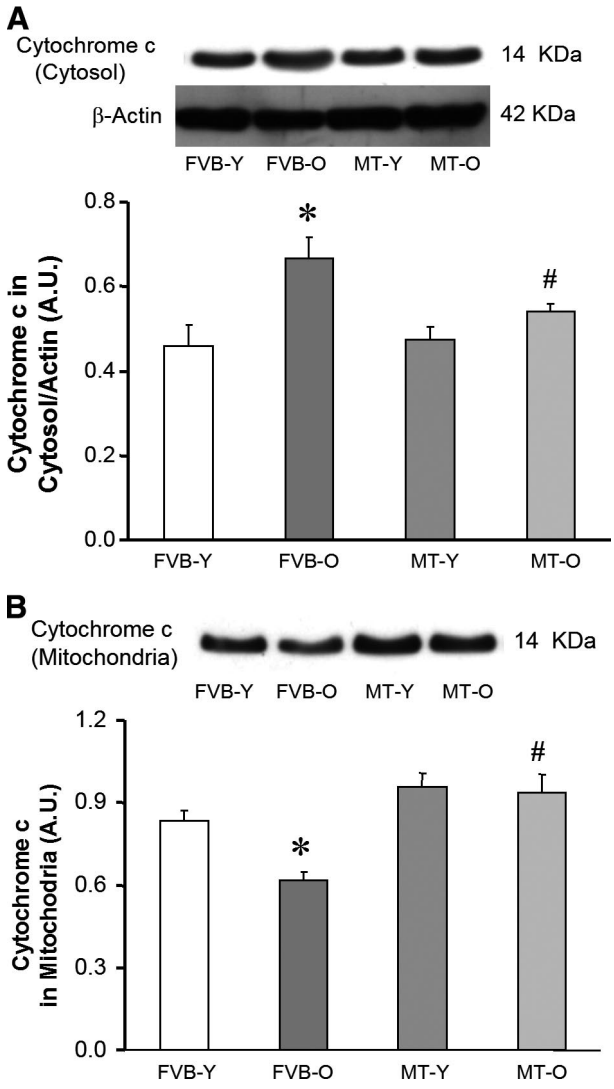

Figure 8. Effect of metallothionein overexpression on cytochrome *c* release in young and aged mouse hearts. Ventricular tissues were separated by differential density centrifugation to yield a membrane fraction (mitochondria) and a soluble fraction (cytosol). *A)* mitochondrial fraction of cytochrome *c* protein expression. Inset: representative immunoblots of cytochrome *c* and β-actin using specific antibodies. *B)* cytosolic fraction of cytochrome *c* protein expression. Mean ± SE; $n = 3$; $^{*}P < 0.05$ vs. FVB-Y group, $^{\#}P < 0.05$ vs. FVB-O group.

Enhanced oxidative stress is commonly found with advanced age (10). It was recently shown that overexpression of the antioxidant catalase, an enzyme known to reduce accumulation of ROS and subsequent oxidative stress, extends murine life span (36). Mitochondria have been speculated as the major site for oxidative stress-induced damage, although mammalian evidence is sparse (39). Our present study revealed that metallothionein, another known free radical scavenger, exerts similar effects against the aging process especially cardiac aging. Accumulation of oxygen free radicals or oxidative stress directly compromises ventricu-

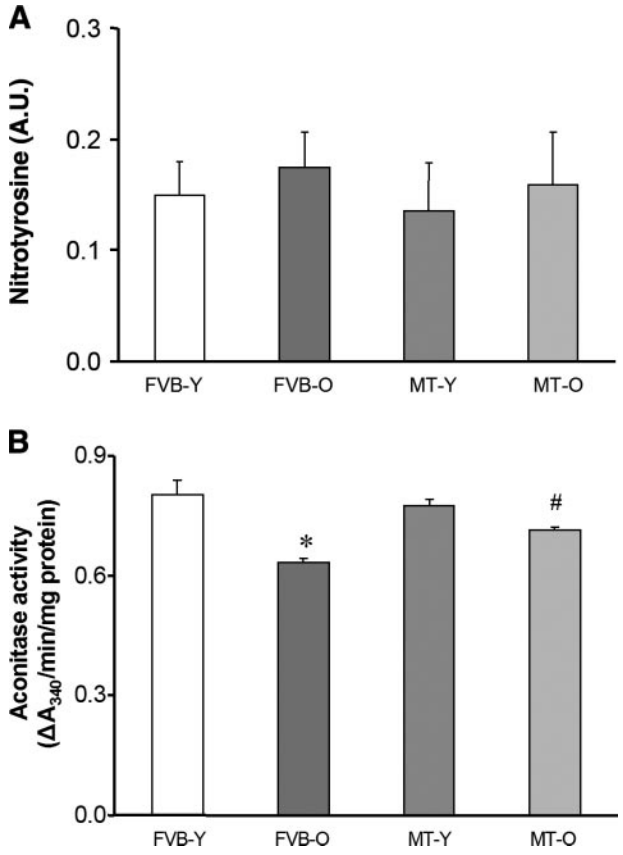

Figure 9. Nitrotyrosine expression (*A*) and mitochondrial aconitase activity (*B*) in heart tissues from young and aged FVB or metallothionein mice. Mean ± SE; $n = 3–6$; $^{*}P < 0.05$ vs. FVB-Y group, $^{\#}P < 0.05$ vs. FVB-O group.

lar function through NADPH oxidase activity, activation of stress signaling molecules, stimulation of renin-angiotensin system, and direct myogenic effects on heart muscles (40–42). Reduction of oxidative stress by either enzymatic or nonenzymatic antioxidants has been shown to improve cardiac function and reduce cardiac apoptosis (9, 43, 44). In the current study, advanced age elicited oxidative stress without hyperglycemia or hypertension, thus excluding contribution of diabetes and hypertension to our aging model. Data from our study revealed that ventricular myocytes from aged FVB mice displayed prolonged relaxation (TR_{90}), while all other mechanical indices (PS, maximal velocity of shortening/relengthening, time-to-PS) were normal. Moreover, aged cardiomyocytes exhibited diminished stress tolerance manifested as significantly reduced PS at higher stimulating frequencies. These data are consistent with our previous findings using murine model (at similar ages) (1). Reduced intracellular Ca^{2+} clearance rate in aged FVB myocytes is in line with prolonged relaxation duration and reduced intracellular Ca^{2+} cycling ability (reduced PS at high stimulating frequencies) in cardiomyocytes from aged animals.

Recent evidence indicates that the small GTPase RhoA participates in the regulation of multiple cell functions, including adhesion, proliferation, migration, and Ca^{2+} homeostasis through kinase cascade activation. The Rho family consists of several members among which RhoA is the most ubiquitously and abundantly expressed in the body. RhoA cycles between two states, an inactive GDP-bound form and an active GTP-bound form that translocates to the membrane where it acts on various effector molecules. Enhanced RhoA activity has been shown to lead to oxidative stress (45,46). Meanwhile, up-regulation of RhoA protein has been reported in aged blood vessels (47). Likewise, our data show RhoA activity is increased in aged cardiomyocytes, and this effect is reduced by metallothionein over-expression. Our observation that the aging-associated cardiomyocyte dysfunction may be ablated by the Rho kinase inhibitor Y-27632 provided further convincing support to the involvement of RhoA in cardiac aging.

The mechanical and intracellular Ca^{2+} defects triggered by advanced age were alleviated by metallothio-

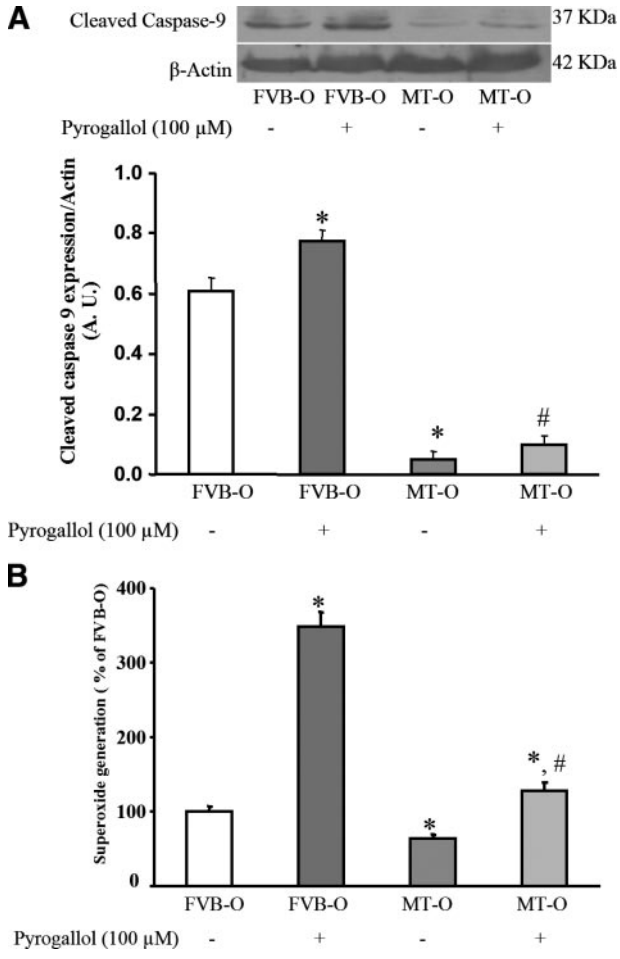

Figure 10. Cleaved caspase-9 expression (*A*) and superoxide generation (*B*) in cardiomyocytes from aged FVB (FVB-O) and metallothionein (MT-O) mice with or without a 2 h incubation of the superoxide generator pyrogallol (100 μM). Superoxide generation was normalized to that of the FVB-O group in the absence of pyrogallol. Means ± SE; $n = 3–6$ samples per group for *A*, and $n = 33$ cells per group for *B*; $^{*}P < 0.05$ vs. pyrogallol absent control or FVB-O group; $^{\#}P < 0.05$ vs. FVB-O group with pyrogallol.

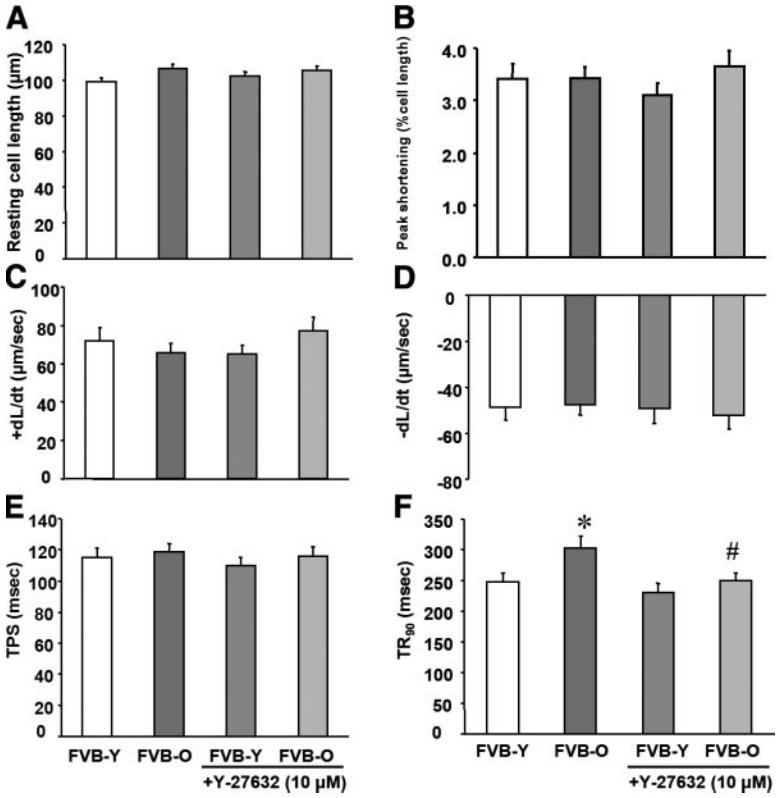

Figure 11. Contractile properties of cardiomyocytes from young and aged FVB mice treated with or without incubation of the Rho kinase inhibitor Y-27632 (10 μM) for 4 h. *A*) Resting cell length. *B*) PS (normalized to cell length). *C*) Maximal velocity of shortening (+dL/d*t*). *D*) Maximal velocity of relengthening (−dL/dt); *E*) Time-to-peak shortening (TPS). *F*) Time-to-90% relengthening (TR_{90}). Mean ± SE; $n = 78$ cells/group; $^{*}P < 0.05$ vs. FVB-Y group alone, $^{\#}P < 0.05$ vs. FVB-O group alone.

nein, in a manner similar to its effect on diabetes-induced cardiac contractile dysfunctions (13). Metallothionein offered protection of cardiomyocyte function in type 1 diabetes and insulin resistance due to its antioxidant action (13,45). This is supported by our present finding in that metallothionein antagonizes aging-induced up-regulation of NADPH oxidase subunit $p47^{phox}$, superoxide generation, and propensity to pyrogallol-induced superoxide generation and apoptosis, as well as other biomarkers of oxidative stress including increased cytochrome *c* release and decreased aconitase activity. The lack of effect on protein nitration suggests that reactive nitrogen species may not be playing a major role in aging-induced cardiac oxidative stress and contractile dysfunction or metallothionein-elicited anti-aging effects. It is also worth mentioning that although aging itself does not trigger a drop in the cardiac metallothionein levels, metallothionein overexpression should help to compensate for the reduced overall antioxidant capacity in aging. We cannot offer any explanation for the age-related increase metallothionein levels in the transgenic mice. It is possible that certain protein-to-protein interaction exists between cardiac senescent proteins and the MHC promoter driving the metallothionein gene. Further study is warranted to elucidate the precise mechanism(s) of aging-related change in antioxidant levels, enhanced oxidative stress, and stress signaling activation in cardiac aging and longevity.

In summary, our data demonstrated that overexpression of metallothionein in the heart could alleviate advanced aging-triggered cardiac contractile defects, while increasing survival, an effect possibly associated with inhibition of NADPH oxidase-mediated superoxide generation, RhoA activation, and enhanced oxidative stress. FJ

The authors are grateful to Dr. Feng Dong, Dr. Shiyan Li, Bonnie H. Zhao, and Matthew S. Stratton for skillful technical assistance. Metallothionein founder mice were kindly provided by Dr. Paul N. Epstein from University of Louisville (Louisville, KY). Helpful discussion with Dr. Lu Cai from University of Louisville (Louisville, KT) is greatly appreciated. This work was supported in part by grants from American Diabetes Association (7–00-RA-21), American Heart Association Pacific Mountain Affiliate (#0355521Z), National Institute of Aging AG21324 (JR) and National Heart Lung and Blood Institute HL66575 (MTQ).

REFERENCES

1. Li, S. Y., Du, M., Dolence, E. K., Fang, C. X., Mayer, G. E., Ceylan-Isik, A. F., LaCour, K. H., Yang, X., Wilbert, C. J., Sreejayan, N., and Ren, J. (2005) Aging induces cardiac diastolic dysfunction, oxidative stress, accumulation of advanced glycation endproducts and protein modification. *Aging Cell* **4,** 57–64
2. Harman, D. (1981) The aging process. *Proc. Natl. Acad. Sci. U. S. A.* **78,** 7124–7128
3. Stadtman, E. R., Starke-Reed, P. E., Oliver, C. N., Carney, J. M., and Floyd, R. A. (1992) Protein modification in aging. *EXS.* **62,** 64–72
4. Sohal, R. S., and Weindruch, R. (1996) Oxidative stress, caloric restriction, and aging. *Science* **273,** 59–63
5. Dhalla, N. S., Temsah, R. M., and Netticadan, T. (2000) Role of oxidative stress in cardiovascular diseases. *J. Hypertens.* **18,** 655–673
6. Dhalla, N. S., and Temsah, R. M. (2001) Sarcoplasmic reticulum and cardiac oxidative stress: an emerging target for heart disease. *Expert Opin. Ther. Targets* **5,** 205–217

7. Harman, D. (1956) Aging: a theory based on free radical and radiation chemistry. *J Gerontol* **11,** 298–300
8. Alexeyev, M. F., Ledoux, S. P., and Wilson, G. L. (2004) Mitochondrial DNA and aging. *Clin. Sci. (Lond)* **107,** 355–364
9. Monahan, K. D., Eskurza, I., and Seals, D. R. (2004) Ascorbic acid increases cardiovagal baroreflex sensitivity in healthy older men. *Am. J. Physiol. Heart Circ. Physiol.* **286,** H2113–2117
10. Yang, X., Sreejayan, N., and Ren, J. (2005) Views from within and beyond: narratives of cardiac contractile dysfunction under senescence. *Endocrine* **26,** 127–137
11. Lakatta, E. G., and Levy, D. (2003) Arterial and cardiac aging: major shareholders in cardiovascular disease enterprises: Part II: the aging heart in health: links to heart disease. *Circulation* **107,** 346–354
12. Cai, L., Wang, J., Li, Y., Sun, X., Wang, L., Zhou, Z., and Kang, Y. J. (2005) Inhibition of superoxide generation and associated nitrosative damage is involved in metallothionein prevention of diabetic cardiomyopathy. *Diabetes* **54,** 1829–1837
13. Ye, G., Metreveli, N. S., Ren, J., and Epstein, P. N. (2003) Metallothionein prevents diabetes-induced deficits in cardiomyocytes by inhibiting ROS production. *Diabetes* **52,** 777–783
14. Kang, Y. J., Chen, Y., Yu, A., Voss-McCowan, M., and Epstein, P. N. (1997) Overexpression of metallothionein in the heart of transgenic mice suppresses doxorubicin cardiotoxicity. *J. Clin. Invest.* **100,** 1501–1506
15. Duan, J., Zhang, H. Y., Adkins, S. D., Ren, B. H., Norby, F. L., Zhang, X., Benoit, J. N., Epstein, P. N., and Ren, J. (2003) Impaired cardiac function and insulin-like growth factor-I response in myocytes from calmodulin-diabetic mice: role of Akt and RhoA. *Am. J. Physiol. Endocrinol. Metab.* **284,** E366–376
16. Hool, L. C., Di Maria, C. A., Viola, H. M., and Arthur, P. G. (2005) Role of NAD(P)H oxidase in the regulation of cardiac L-type Ca2+ channel function during acute hypoxia. *Cardiovasc Res.* **67,** 624–635
17. Esberg, L. B., and Ren, J. (2004) The oxygen radical generator pyrogallol impairs cardiomyocyte contractile function via a superoxide and p38 MAP kinase-dependent pathway: protection by anisodamine and tetramethylpyrazine. *Cardiovasc Toxicol.* **4,** 375–384
18. Dong, F., Zhang, X., Culver, B., Chew, H. G., Kelley, R. O., and Ren, J. (2005) Dietary iron deficiency induces ventricular dilation, mitochondrial ultrastructural aberrations and cytochrome c release: involvement of nitric oxide synthase and protein tyrosine nitration. *Clin. Sci. (Lond)* **109,** 277–286
19. DeLeo, F. R., Nauseef, W. M., Jesaitis, A. J., Burritt, J. B., Clark, R. A., and Quinn, M. T. (1995) A domain of p47phox that interacts with human neutrophil flavocytochrome b558. *J. Biol. Chem.* **270,** 26246–26251
20. Song, Y., Wang, J., Li, Y., Du, Y., Arteel, G. E., Saari, J. T., Kang, Y. J., and Cai, L. (2005) Cardiac metallothionein synthesis in streptozotocin-induced diabetic mice, and its protection against diabetes-induced cardiac injury. *Am. J. Pathol.* **167,** 17–26
21. Dong, F., Zhang, X., Wold, L. E., Ren, Q., Zhang, Z., and Ren, J. (2005) Endothelin-1 enhances oxidative stress, cell proliferation and reduces apoptosis in human umbilical vein endothelial cells: role of ETB receptor, NADPH oxidase and caveolin-1. *Br. J. Pharmacol.* **145,** 323–333
22. Yarian, C. S., Rebrin, I., and Sohal, R. S. (2005) Aconitase and ATP synthase are targets of malondialdehyde modification and undergo an age-related decrease in activity in mouse heart mitochondria. *Biochem. Biophys. Res. Commun.* **330,** 151–156
23. Kawamura, H., Yokote, K., Asaumi, S., Kobayashi, K., Fujimoto, M., Maezawa, Y., Saito, Y., and Mori, S. (2004) High Glc-induced upregulation of osteopontin is mediated via Rho/Rho kinase pathway in cultured rat aortic smooth muscle cells. *Arterioscler. Thromb. Vasc. Biol.* **24,** 276–281
24. Chung, L., and Ng, Y. C. (2005) Age-related alterations in expression of apoptosis regulatory proteins and heat shock proteins in rat skeletal muscle. *Biochim. Biophys. Acta* **1762,** 103–109
25. Kurosu, H., Yamamoto, M., Clark, J. D., Pastor, J. V., Nandi, A., Gurnani, P., McGuinness, O. P., Chikuda, H., Yamaguchi, M., Kawaguchi, H., Shimomura, I., Takayama, Y., Herz, J., Kahn, C. R., Rosenblatt, K. P., and Kuro-o, M. (2005) Suppression of aging in mice by the hormone Klotho. *Science* **309,** 1829–1833
26. Bindokas, V. P., Jordan, J., Lee, C. C., and Miller, R. J. (1996) Superoxide production in rat hippocampal neurons: selective imaging with hydroethidine. *J. Neurosci.* **16,** 1324–1336
27. Cai, H., Griendling, K. K., and Harrison, D. G. (2003) The vascular NAD(P)H oxidases as therapeutic targets in cardiovascular diseases. *Trends Pharmacol. Sci.* **24,** 471–478
28. Wang, G. W., Schuschke, D. A., and Kang, Y. J. (1999) Metallothionein-overexpressing neonatal mouse cardiomyocytes are resistant to H2O2 toxicity. *Am. J. Physiol.* **276,** H167–175
29. Cai, L., and Kang, Y. J. (2001) Oxidative stress and diabetic cardiomyopathy: a brief review. *Cardiovasc Toxicol.* **1,** 181–193
30. Jin, L., Ying, Z., and Webb, R. C. (2004) Activation of Rho/Rho kinase signaling pathway by ROS in rat aorta. *Am. J. Physiol. Heart Circ. Physiol.* **287,** H1495–1500
31. Rikitake, Y., and Liao, J. K. (2005) Rho-kinase mediates hyperglycemia-induced plasminogen activator inhibitor-1 expression in vascular endothelial cells. *Circulation* **111,** 3261–3268
32. Luo, J. D., and Chen, A. F. (2003) Perspectives on the cardioprotective effects of statins. *Curr. Med. Chem.* **10,** 1593–1601
33. Ren, J., and Fang, C. X. (2005) Small guanine nucleotide-binding protein Rho and myocardial function. *Acta Pharmacol. Sin.* **26,** 279–285
34. Matsuoka, Y., Picciano, M., La Francois, J., and Duff, K. (2001) Fibrillar beta-amyloid evokes oxidative damage in a transgenic mouse model of Alzheimer's disease. *Neuroscience* **104,** 609–613
35. Yan, L. J., Levine, R. L., and Sohal, R. S. (1997) Oxidative damage during aging targets mitochondrial aconitase. *Proc. Natl. Acad. Sci. U. S. A.* **94,** 11168–11172
36. Schriner, S. E., Linford, N. J., Martin, G. M., Treuting, P., Ogburn, C. E., Emond, M., Coskun, P. E., Ladiges, W., Wolf, N., Van Remmen, H., Wallace, D. C., and Rabinovitch, P. S. (2005) Extension of murine life span by overexpression of catalase targeted to mitochondria. *Science* **308,** 1909–1911
37. Gardner, P. R., and Fridovich, I. (1992) Inactivation-reactivation of aconitase in Escherichia coli. A sensitive measure of superoxide radical. *J. Biol. Chem.* **267,** 8757–8763
38. Kanda, T., Wakino, S., Homma, K., Yoshioka, K., Tatematsu, S., Hasegawa, K., Takamatsu, I., Sugano, N., Hayashi, K., and Saruta, T. (2005) Rho-kinase as a molecular target for insulin resistance and hypertension. *FASEB J.* In press
39. Fridovich, I. (2004) Mitochondria: are they the seat of senescence? *Aging Cell* **3,** 13–16
40. Benderdour, M., Charron, G., Comte, B., Ayoub, R., Beaudry, D., Foisy, S., Deblois, D., and Des Rosiers, C. (2004) Decreased cardiac mitochondrial NADP+-isocitrate dehydrogenase activity and expression: a marker of oxidative stress in hypertrophy development. *Am. J. Physiol. Heart Circ. Physiol.* **287,** H2122–2131
41. Benderdour, M., Charron, G., DeBlois, D., Comte, B., and Des Rosiers, C. (2003) Cardiac mitochondrial NADP+-isocitrate dehydrogenase is inactivated through 4-hydroxynonenal adduct formation: an event that precedes hypertrophy development. *J. Biol. Chem.* **278,** 45154–45159
42. Ceconi, C., Boraso, A., Cargnoni, A., and Ferrari, R. (2003) Oxidative stress in cardiovascular disease: myth or fact? *Arch Biochem. Biophys.* **420,** 217–221
43. Xu, Y., Armstrong, S. J., Arenas, I. A., Pehowich, D. J., and Davidge, S. T. (2004) Cardioprotection by chronic estrogen or superoxide dismutase mimetic treatment in the aged female rat. *Am. J. Physiol. Heart Circ. Physiol.* **287,** H165–171
44. Kasapoglu, M., and Ozben, T. (2001) Alterations of antioxidant enzymes and oxidative stress markers in aging. *Exp. Gerontol.* **36,** 209–220
45. Fang, C. X., Dong, F., Ren, B. H., Epstein, P. N., and Ren, J. (2005) Metallothionein alleviates cardiac contractile dysfunction induced by insulin resistance: role of Akt phosphorylation, PTB1B, PPARgamma and c-Jun. *Diabetologia* **48,** 2412–2421
46. Sowers, J. R. (2004) Insulin resistance and hypertension. *Am. J. Physiol. Heart Circ. Physiol* **286,** H1597–1602
47. Miao, L., Calvert, J. W., Tang, J., Parent, A. D., and Zhang, J. H. (2001) Age-related RhoA expression in blood vessels of rats. *Mech. Ageing Dev.* **122,** 1757–1770

Received for publication October 17, 2005.
Accepted for publication December 19, 2005.